EPJ Web of Conferences **137**, 01001 (2017) DOI: 10.1051/epjconf/201713701001
XIIth Quark Confinement & the Hadron Spectrum

Round table: Flavour anomalies in $b \to s\ell^+\ell^-$ processes

T. Blake[1], M. Gersabeck[2,a], L. Hofer[3], S. Jäger[4], Z. Liu[5], and R. Zwicky[6]

[1] *University of Warwick, Coventry, UK*
[2] *The University of Manchester, Manchester, UK*
[3] *Institut de Ciencies del Cosmos, Universitat de Barcelona, Barcelona, Spain*
[4] *University of Sussex, Brighton, UK*
[5] *Institute of High Energy Physics and Theoretical Physics Center for Science Facilities, Chinese Academy of Sciences, Beijing, 100049, China*
[6] *University of Edinburgh, Edinburgh, UK*

Abstract. Precision measurements of flavour observables can provide powerful tests of many extensions of the Standard Model. This contribution covers a range of flavour measurements of $b \to s\ell^+\ell^-$ transitions, several of which are in tension with the Standard Model of particle physics, as well as their theoretical interpretation. The basics of the theoretical background are discussed before turning to the main question of the field: whether the anomalies can be explained by QCD effects or whether they may be indicators of effects beyond the Standard Model.

1 Introduction

Flavour physics has a long track record of discoveries that paved the way for advances in particle physics. In particular the discovery of B^0 meson oscillations in 1987 [1] is a great example to demonstrate the potential of flavour physics to infer physics of high mass scales through precision measurements at low scales: the observed rate of oscillations was the first indication of the top quark being much heavier than the other five quark flavours. Precision flavour measurements at the LHC are sensitive to indirect effects from physics beyond the Standard Model (SM) at far greater scales than those accessible in direct searches.

A particular sensitive class of processes are those undergoing a $b \to s\ell^+\ell^-$ transition. This paper summarises a panel discussion focussing on a range of anomalies seen in measurements of decays of this type. Section 2 reviews the experimental situation, followed by Sec. 3, which covers the basics of rare B decays in the context of the heavy quark expansion. The central discussion around the observed anomalies is whether these are indeed beyond the SM (BSM) effects or whether they can be explained by QCD effects. Section 4 discusses light-cone sum rules and lattice form-factor determinations relevant for exclusive $b \to s\ell^+\ell^-$ transitions. Charm loops are analysed in Sec. 5. Section 6 describes global fits that aim to combine experimental observables to extract a more precise theoretical picture. Finally, Sec. 7 covers potential BSM interpretations of the flavour anomalies before the summary, which is given in Sec. 8.

[a] e-mail: Marco.Gersabeck@cern.ch

2 Summary of experimental situation (T. Blake)

There has been huge experimental progress in measurements of rare $b \to s$ processes in the past five years. This has been driven by the large $b\bar{b}$ production cross-section in pp collisions at the LHC, which enabled the LHC experiments to collect unprecedented samples of decays with dimuon final-states.

2.1 Leptonic decays

The decay $B_s^0 \to \mu^+\mu^-$ is considered a golden mode for testing the SM at the LHC. The SM branching fraction depends on single hadronic parameter, the B_s^0 decay constant, that be computed from Lattice CQD. Consequently the SM branching fraction is known to better than a 10% precision [2]. A combined analysis of the CMS and LHCb datasets [3] results in a time-averaged measurement of the branching fraction of the decay of

$$\overline{\mathcal{B}}(B_s^0 \to \mu^+\mu^-) = (2.8^{+0.7}_{-0.6}) \times 10^{-9} \,. \tag{1}$$

A recent ATLAS measurement [4] yields

$$\overline{\mathcal{B}}(B_s^0 \to \mu^+\mu^-) = (0.9^{+1.1}_{-0.8}) \times 10^{-9} \,, \tag{2}$$

which is consistent with the combined analysis from CMS and LHCb. These measurements are in good agreement with SM predictions and sets strong constraints on extensions of the SM that introduce new scalar or pseudoscalar couplings.

2.2 Semileptonic decays

The large dataset has also enabled the LHCb and CMS experiments to make the most precise measurements of the differential branching fraction of $B \to K^{(*)}\mu^+\mu^-$ and $B_s^0 \to \phi\mu^+\mu^-$ to date [5–7]. Above the open charm threshold, broad resonances are seen in the LHCb dataset [8]. The most prominent of these is the $\psi(4160)$. The regions close to the narrow charmonium resonances are excluded from the analysis. With the present binning scheme, the uncertainties on differential branching fraction measurements are limited by the knowledge of the $B \to J/\psi K^{(*)}$ and $B_s^0 \to J/\psi\phi$ branching fractions that are used to normalise the signal. The measured differential branching fractions of $b \to s\mu^+\mu^-$ processes, tend to prefer smaller values than their corresponding SM predictions. The largest discrepancy is seen in the $B_s^0 \to \phi\mu^+\mu^-$ decay, where the data are more than $3\,\sigma$ from the SM predictions in the dimuon invariant mass squared range $1 < q^2 < 6\,\mathrm{GeV}^2/c^4$, see Fig 1.

While the branching fractions of rare $B \to K^{(*)}\mu^+\mu^-$ decays have large theoretical uncertainties arising from the $B \to K^{(*)}$ form-factors, many sources of uncertainty will cancel when comparing the decay rates of the $B \to K^{(*)}\mu^+\mu^-$ and $B \to K^{(*)}e^+e^-$ decays. In the range $1 < q^2 < 6\,\mathrm{GeV}^2/c^4$, the LHCb experiment measures [12]

$$R_K[1,6] = 0.745\,^{+0.090}_{-0.074}(\mathrm{stat})\,^{+0.035}_{-0.035}(\mathrm{syst}) \,. \tag{3}$$

This is approximately $2.6\,\sigma$ from the SM expectation of almost identical decay rates for the two channels. In order to cancel systematic differences between the reconstruction of electrons and muons in the detector, the LHCb analysis is performed as a double ratio to the rate $B^+ \to J/\psi K^+$ decays (where the J/ψ can decay to a dielectron or dimuon pair). The migration of events in q^2 due to

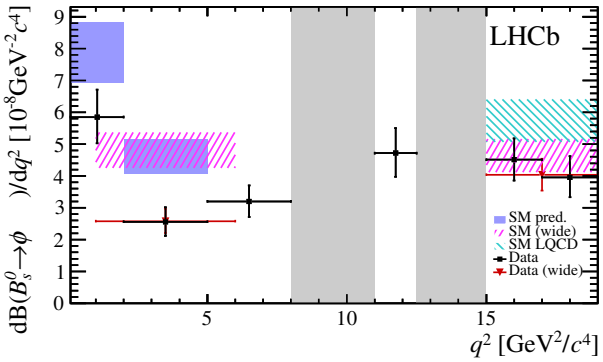

Figure 1. Differential branching fraction of the $B_s^0 \to \phi\mu^+\mu^-$ decay measured by the LHCb experiment [6] as a function of the dimuon invariant mass squared, q^2. The data are compared to SM predictions based on Refs. [9, 10] and [11]. The rise in the branching fraction at low q^2 arises from virtual photon contributions to the decay. Reproduced from Ref. [6].

final-state-radiation is accounted for using samples of simulated events. QED effects are simulated through PHOTOS [13]. The largest difference between the dimuon and dielectron final-states comes from Bremsstrahlung from the electrons in the detector. This is simulated using GEANT 4 [14]. The modelling of the migration of events and the line-shape of the decay are the main contributions to the systematic uncertainty on the measurement.

The distribution of the final-state particles in the $B \to K^*\ell^+\ell^-$ decay can be described by three angles and q^2. The angles are: the angle between the direction of the ℓ^+ (ℓ^-) and the B ($\bar{B}$) in the rest-frame of the dilepton pair; the angle between the direction of the kaon and the direction of the B in the K^* rest-frame; and the angle between the decay planes of the dilepton pair and the K^* in the rest-frame of the B, denoted ϕ. The resulting angular distribution can be parameterised in terms of eight angular observables: the longitudinal polarisation of the K^*, $F_{\rm L}$; the forward-backward asymmetry of the dilepton system, $A_{\rm FB}$; and six additional observables that cancel when integrating over ϕ. Existing measurements of the observables $A_{\rm FB}$ and $F_{\rm L}$ are shown in Fig. 2 along with SM predictions based on Refs. [9, 10]. The most precise measurements of the $F_{\rm L}$ and $A_{\rm FB}$ come from the LHCb and CMS experiments. In general, the measurements are consistent with each other and are compatible with the SM predictions. The largest tension is seen in the BaBar measurement of $F_{\rm L}$ [15].

The LHCb and Belle experiments have also measured the remaining angular observables that are usually cancelled by integrating over ϕ. For the first time, LHCb has also performed a full angular analysis of the decay [18]. The majority of these additional observables are consistent with SM predictions. However, a tension exists between measurements of the observable P_5' and their corresponding SM prediction in the region $4 < q^2 < 8\,{\rm GeV}^2/c^4$. This tension is illustrated in Fig. 3. In the region $4 < q^2 < 8\,{\rm GeV}^2/c^4$, the data are significantly above the SM predictions.

The experimental measurements of the angular observables are currently statistically limited. The largest sources of systematic uncertainty arise from modelling of the experiments angular acceptance and the background angular distribution.

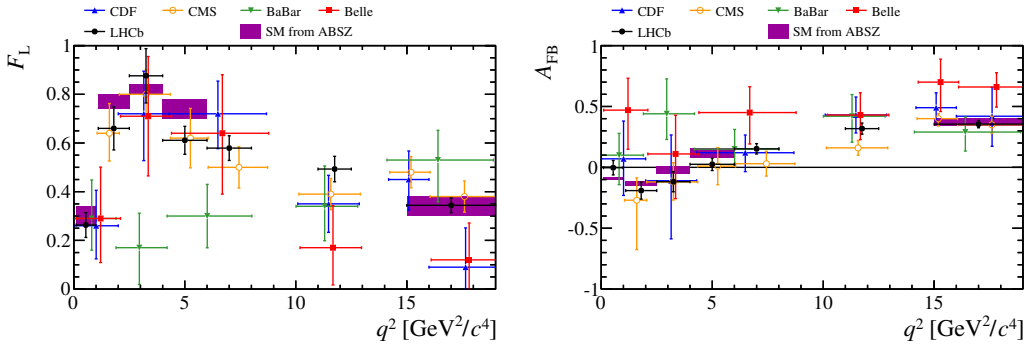

Figure 2. Observables F_L and A_{FB} measured by the BaBar [15], Belle [16], CDF [17], CMS [7] and LHCb [18] experiments for the $B \to K^*\mu^+\mu^-$ decay as a function of the dimuon invariant mass squared, q^2. The shaded region indicates a theoretical prediction for the observables based on Refs. [9, 10]. No data point is shown for CMS in the range $q^2 < 1\,\text{GeV}^2/c^4$, due to the thresholds used in the CMS trigger system.

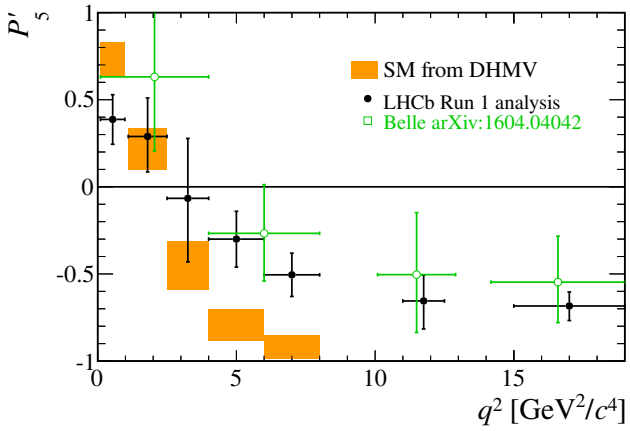

Figure 3. Observable P'_5 measured by LHCb [18] and Belle [19] as a function of the dimuon invariant mass squared, q^2, in the $B \to K^*\mu^+\mu^-$ decay. The shaded regions indicate theoretical predictions from Ref. [20].

3 Rare B-decays and the heavy quark expansion (S. Jäger)

3.1 Context

In the Standard Model (SM), the amplitude for a rare semileptonic decay $\bar{B} \to M\ell^+\ell^-$, with M a hadronic system such as $\bar{K}$, $\bar{K}\pi, \ldots$ can be written, to leading order in the electromagnetic coupling α_{EM} but exact in QCD, as

$$\mathcal{A}(B \to M\ell^+\ell^-) = L^\mu a_{V\mu} + L^{5\mu} a_{A\mu}, \tag{4}$$

where L^μ and $L^{5\mu}$ are the vector and axial lepton currents. One can trade $a_{V\mu}$, $a_{A\mu}$ for helicity amplitudes $H_{V\lambda}(q^2)$ and $H_{A\lambda}(q^2)$, where λ is the helicity of the dilepton, which coincides with that of the hadronic state. For a kaon, $\lambda = 0$ and there are two hadronic amplitudes. For a narrow K^*, $\lambda = \pm 1$

and there are six amplitudes.[1] These amplitudes determine all rate and angular observables measured at B-factories and LHCb (where the lepton spins are not measured).

In the conventions of [21], $H_{A\lambda} \propto C_{10} V_\lambda(q^2)$, where V_λ are form factors and C_{10} is the axial semileptonic Wilson coefficient. (We omitted a normalisation free of hadronic uncertainties.) Note that C_{10} and V_λ are renormalisation-scale and -scheme-independent. C_{10}, in fact, receives no contributions from below the weak scale at all. The vector amplitudes can be written [21]

$$H_{V\pm} \propto \left[C_9(\mu) V_\pm(q^2) + \frac{2 m_b m_B}{q^2} C_7^{\rm eff}(\mu) T_\pm(q^2,\mu) - 16\pi^2 \frac{m_B^2}{q^2} h_\pm(q^2,\mu) \right], \tag{5}$$

$$H_{V0} \propto \frac{\lambda^{1/2}}{2 m_B \sqrt{q^2}} \left[C_9(\mu) V_0(q^2) + \frac{2 m_b}{m_B} C_7^{\rm eff}(\mu) T_0(q^2,\mu) \right] - 16\pi^2 \frac{m_B^2}{q^2} h_0(q^2,\mu). \tag{6}$$

Here $C_9(\mu)$ denotes the vector semileptonic Wilson coefficient, T_λ tensor form factors, multiplied by the "effective" dipole Wilson coefficient $C_7^{\rm eff}$, and $h_\lambda \sim \langle M(\lambda)|T\left\{ j^{\rm em,had}(y) \mathcal{H}_{\rm had}^{\rm eff}(0) \right\}|\bar{B}\rangle$ denotes the contribution from the hadronic weak Hamiltonian (see [21] for a precise definition). So far everything is exact from a QCD point of view. The theoretical difficulty resides in the evaluation of h_λ, which the heavy-quark expansion achieves, and of the form factors, for which the heavy-quark expansion provides relations.

One notes that $C_9(\mu)$ and $C_7^{\rm eff}(\mu)$ are strongly scale-dependent. E.g., at NNLL order, $C_9(10{\rm GeV}) = 3.75$, $C_9(5{\rm GeV}) = 4.18$, $C_9(2.5{\rm GeV}) = 4.49$. (One may compare this variation to a putative $\Delta C_9^{\rm BSM} \sim -1$.) The scale dependence must be precisely cancelled by the non-perturbative object h_λ. (This follows from RG-invariance of the Hamiltonian, which is exact.) Any quantitative theoretical description of h_λ must correctly incorporate this.[2]

3.2 The heavy-quark expansion

In the heavy-quark, large-recoil limit $E_M, m_B \gg \Lambda$, where Λ is the QCD scale parameter, h_λ factorizes into perturbative hard-scattering kernels multiplying form factors and light-cone distribution amplitudes for the light meson $M = K, K^*$ [23–25], known as QCD factorization. It applies in the q^2-region below the narrow charm resonances, and perhaps above the charm threshold up to $q^2 \sim 15{\rm GeV}^2$. QCDF can be formulated in soft-collinear effective field theory (SCET) language [26]. "Factorization" is used in the Wilsonian sense of separating physics of the scales $\sqrt{\Lambda m_b}$, m_b, and above from the physics of the scale Λ, not to be confused with "naive factorization." There are two distinct classes of effects. Vertex corrections may be compactly written as

$$C_9 \quad \to \quad C_9(\mu) + Y(\mu, q^2, m_c) + \frac{\alpha_s}{4\pi} Y^{(1)}(\mu, q^2, m_c), \tag{7}$$

$$C_7^{\rm eff} \quad \to \quad C_7^{\rm eff}(\mu) + \frac{\alpha_s}{4\pi} Z^{(1)}(\mu, q^2, m_c), \tag{8}$$

where $Y, Y^{(1)}$,and $Z^{(1)}$ contain loop functions and Wilson coefficients. This form makes the helicity independence of these effects evident. The combination $C_9 + Y$ is traditionally called $C_9^{\rm eff}(q^2)$; the heavy-quark limit justifies its use, but also predicts model-independent higher-order corrections. (Note that C_9 starts at $O(1/\alpha_s)$ in the logarithmic counting, so Y is formally a NLL correction.) The

[1] We neglect the lepton mass, as the anomalies occur at $q^2 \gg m_\ell^2$. This eliminates a seventh amplitude. We will also neglect the strange quark mass and CKM-suppressed terms throughout.

[2] A recent LHCb paper [22] models h_λ, for $B \to K$, as a sum of Breit-Wigner resonances. While this more or less fits the data ($p \approx 0.01$), it has no scale-dependence, which is one reason why the coefficient C_9 in that paper cannot be identified with $C_9(\mu)$ for any scale μ.

r.h.s. of (7),(8) are μ-independent up to $O(\alpha_s^2)$ corrections. The other class of effects constitutes so-called hard spectator scattering and includes an annihilation contribution at $O(\alpha_s^0)$, though the latter comes with small CKM-factors and Wilson coefficients. Spectator scattering probes the structure of the B and K^*-mesons through their light-cone distribution amplitudes and is helicity dependent (and vanishes for $\lambda = +$). Schematically,

$$h_\lambda^{\text{spec}} \propto T_\lambda(\alpha_s) * \phi_{B_\pm} * \phi_{K^*}. \tag{9}$$

This expression is separately scale-independent, resulting in formally μ-independent observables. Corrections to the heavy-quark limit scale like Λ/m_B and do not factorize, and must be estimated in other ways.

The expressions so far are sufficient to express all observables in terms of form factors [27], one can then use form factor results from light-cone sum rules to compute observables. Alternatively, one can make use of the fact that the heavy-quark large-recoil limit also implies relations between different form factors [28–30]. They look extremely simple in the helicity basis,

$$T_\lambda(q^2) = V_\lambda(q^2)[1 + f_\lambda(q^2, \alpha_s)] + \text{spectator scattering} + O(\Lambda/m_B) \tag{10}$$

for $\lambda = -, 0$ and $T_+(q^2) = V_+(q^2) = O(\Lambda/m_B)$. (The latter together with $h_+ = 0$ implies $H_{V+} = H_{A+} = 0$.) Here f_λ is a perturbative expression starting at $O(\alpha_s)$. The spectator-scattering contribution has a form similar to (9), and is again proportional to α_s. All $O(\alpha_s^2)$ corrections are also known [31–34]. Note that the ratios T_λ/V_λ are free of hadronic input in the heavy-quark limit, up to (calculable) spectator-scattering and (incalculable) power corrections.

There is an alternative expansion, applicable at $M_B^2, q^2 \gg \Lambda^2$, in particular above the $D\bar{D}$ threshold. The actual expansion is in $E_M/\sqrt{q^2}$ and expresses h_λ in terms of matrix elements of local operators (OPE) of increasing dimension, again with perturbatively calculable coefficients [35–37]. This is not by itself a heavy-quark expansion, although the kinematics ensure that a HQE is valid and the b-quark field may be expanded accordingly [36], and the HQE can be used to estimate the matrix elements [37]. The leading matrix elements are again the form factors T_λ and V_λ, with perturbative coefficient functions that coincide with C_7^{eff} and $C_9^{\text{eff}}(q^2)$ but different α_s-corrections. The leading higher-dimensional corrections are of order Λ^2/q^2 and negligible, in particular spectator scattering is (strongly) power-suppressed. The OPE also gives a qualitative picture how open-charm resonances arise, by means of analytic continuation of OPE remainder terms from spacelike to physical (timelike) q, $\exp(-c\sqrt{-q^2}/\Lambda) \to \exp(-ic\sqrt{q^2}/\Lambda)$, giving oscillatory behaviour. Note that these "duality-violating" terms are nonanalytic in Λ, hence the large-recoil Λ/m_B expansion will not capture them either. Formally such terms are of "infinite order" in $\Lambda/\sqrt{q^2}$ or Λ/m_B. They become less important away from the threshold and partly cancel out in binned observables (see [37, 38]).

3.3 Phenomenology

How large are the various effects and residual uncertainties? The shift to C_7^{eff} is an $O(25\%)$ constructive correction. The $O(\alpha_s)$ correction to C_9 is an order 5% destructive effect which partly cancels the $O(\alpha_s^0)$ term i.e. $Y(q^2)$. The spectator-scattering corrections are smaller, though the normalisation is quite uncertain (by about a factor of two) due to the poor knowledge of the B-meson LCDA ϕ_{B_+}. Overall the effects are significant. For instance, $\lim_{q^2\to 0}[q^2 H_{V-}(q^2)]$ gives the $B \to K^*\gamma$ amplitude, which receives a +30% correction, or a +70% correction at the rate level. Because C_7^{eff} is tightly constrained from the measured $B \to X_s\gamma$ rate, this allowed [23] to conclude that, absent large power corrections, $T_-(0) = T_1(0) = 0.27 \pm 0.04$, updated to $T_1(0) = 0.28 \pm 0.02$ in [25] and well below LCSR

predictions at the time. A recent LCSR evaluation [10] gives $T_1(0) = 0.308 \pm 0.031$. The consistency supports smallness of power corrections.

It is impossible to give a comprehensive phenomenology of angular $B \to K^*\mu^+\mu^-$ observables in this space. Two observables that are very sensitive to C_9 are the forward-backward asymmetry, specifically its zero-crossing, and the angular term S_5 (or P_5'). As long as Wilson coefficients are real, the FBAS zero is determined by $\mathrm{Re}\, H_{V-}(q_0^2) = 0$, up to *second-order* power corrections $O(\Lambda^2/m_B^2)$. From (5) it is clear that the zero depends on $(C_7^{\mathrm{eff}}/C_9) \times (T_-/V_-)$, essentially free from form-factor uncertainties in the heavy-quark limit. Given the fact that C_7^{eff} is essentially pinned to its SM value by $B \to X_s\gamma$, a q_0^2-measurement may hence be viewed as a determination of C_9. Ref. [25] obtained $q_0^2 = 4.36^{+0.33}_{-0.31}\ \mathrm{GeV}^2$ (neglecting power corrections), to be compared to the LHCb determination [18] $q_0^2 \in [3.40, 4.87]\ \mathrm{GeV}^2$, in good agreement. By comparison, the LCSR form factors of [10] imply a lower crossing point, around 3.5 GeV^2, giving a slight preference for $C_9 < C_9^{\mathrm{SM}}$. This can be traced to a ratio of T_-/V_- that is $O(10\%)$ below the heavy-quark-limit prediction, which is still consistent with a power correction. The eventual relative accuracy on C_9 is limited by that on ratio $T_-(q_0^2)/V_-(q_0^2)$.

The observable P_5' [39], which shows the most pronounced anomaly, depends on all six helicity amplitudes. It hence depends on ratios T_-/V_-, T_0/V_0, V_+/V_-, T_+/V_-, and V_0/V_-. The last of these does not satisfy a heavy-quark relation, but P_5' has been constructed in such a way that dependence on it cancels in the heavy-quark limit if α_s-corrections are neglected. It has been suggested to employ $V \propto V_+ + V_-$ instead of V_- [20], which reduces the explicit sensitivity to V_+ in P_5'. From a pure heavy-quark perspective, the physics of V_+ (which involves soft physics flipping the helicity of the strange quark emitted from b-quark decay, or changing the helicity of the B-remnant absorbed into the K^*) and V_- (which does not require such a spin-flip) seem very different, such that the conservative choice is to associate separate uncertainties to both (hence a larger one to V). The impact on the significance of the P_5' anomaly is noticeable because of this [20, 40] and because [20] adopt central values for power corrections to match LCSR form factor central values while [40] use zero central values (the HQ limit).

3.4 Discussion

The heavy-quark expansion goes a long way to putting rare and rare B decays on a systematic theoretical footing, and rightly has found its place at the heart of many phenomenological works and fits to BSM effects. In particular it removes most of the ambiguities of older "$C_{7,9,10}$ + resonances" approaches. Its primary limitation are incalculable power corrections. There is no evidence that these are abnormally large. Rather, the fact that they matter in the interpretation of anomalies points to the impressive precision that experiment has already reached (and the apparent smallness of possible BSM effects). At the moment, there is no first-principles method to compute power corrections. Light-cone sum rule calculations can provide information. As they carry their own uncontrolled systematics, it would be particularly desirable to have sum rule results *directly* for the power-suppressed terms, where possible. Combining these with the leading-power expressions would remove most of the systematics of either framework. One example is the sum rule [41] for $h_+(q^2)$, which vanishes in the heavy-quark limit. One finds an extra (ie double) power suppression of this term at $q^2 \approx 0$, which implies an excellent sensitivity to C_7' [21, 40]. Data-driven approaches may be able to constrain some of the power corrections, especially if data in very small bin-sizes becomes available for $B \to K^*\mu^+\mu^-$. This path has been followed to some extent in [42].

4 Form factors (Z.Liu & R.Zwicky)

Form factors (FFs) describe the short-distance part of the transition amplitudes. For hadronic transitions of the type $B \to M$ at the quark level $b \to q$ they consist of matrix elements of the form $\langle M(p)|\bar{s}\Gamma b|\bar{B}(p_B)\rangle$ which can be computed from light-cone sum rules (LCSR) and lattice QCD at low and high momentum transfer $q^2 = (p_B - p)^2$ respectively. The most relevant ones to the current discussion of flavour anomalies are the $B \to V$ FFs

$$\begin{aligned}\langle K^*(p,\eta)|\bar{s}\gamma^\mu(1\mp\gamma_5)b|\bar{B}(p_B)\rangle &= P_1^\mu \mathcal{V}_1(q^2) \pm P_2^\mu \mathcal{V}_2(q^2) \pm P_3^\mu \mathcal{V}_3(q^2) \pm P_P^\mu \mathcal{V}_P(q^2)\,,\\ \langle K^*(p,\eta)|\bar{s}iq_\nu\sigma^{\mu\nu}(1\pm\gamma_5)b|\bar{B}(p_B)\rangle &= P_1^\mu T_1(q^2) \pm P_2^\mu T_2(q^2) \pm P_3^\mu T_3(q^2)\,,\end{aligned} \tag{11}$$

corresponding to the vector (e.g. $O_{9,10}$) and tensor current operators (e.g. O_7) and $\mathcal{V}_{1,2,3,P}$ are related to the more commonly known FFs V, $A_{2,3,0}$ FFs [10]. The Lorentz structures $P_{1,2,3,P}$ are functions of p and the polarisation vector η [10]. Below we summarise the status of these computations in LCSR & lattice, discuss the issue of the finite K^*-width and the use of the equation of motion (EOM) on controlling uncertainties. The uncertainty of individual FFs is around 10% but as a result of the correlations uncertainties of ratios can be considerably smaller which is relevant for $B \to K^*\mu\mu$-decays. Pseudo-data are generated using the analytic LCSR computation with a Markov chain process. The resulting distribution is then fitted to a z-series expansion with flat priors on the coefficients [10]. The lattice FFs themselves are fitted to the same expansion including a full error correlation matrix [11]. In addition, a fit interpolating between the LCSR and lattice results is provided [10].

4.1 Status of LCSR and lattice computations

LCSR are computed from a light-cone OPE, valid at $q^2 \leq O(m_b\Lambda) \simeq 14\,\text{GeV}^2$, in an α_s- and twist-expansion which resulting in a convolutions of a hard kernel and light-cone distribution amplitudes (LCDA). The LCDAs are related by EOMs and well-approximated by the first few terms in the conformal partial wave expansion (e.g. Gegenbauer moments). For the $B \to V$ ($B_{(q,s)} \to (K^*, \phi, \rho, \omega)$), defined in (11), the FFs are known up to twist-3 at $O(\alpha_s^3)$ and twist-4 $O(\alpha_s^0)$ [10, 43].[3] State of the art computations of $B \to K$ LCSR FFs, for which the DAs are better known because of the absence of finite width effects, can be found in [41, 45].

Lattice QCD calculations are based on the path integral formalism in Euclidean space. The QCD theory is discretized on a finite space time lattice. Correlation functions, from which FFs can be extracted, are then obtained by solving the integrals numerically using Monte Carlo methods. Since both the noise to signal ratio of correlation functions and discretization effects increase as the momenta of hadrons increase, lattice QCD results cover the high q^2 region at $\sim 15\ \text{GeV}^2 \leq q^2 \leq q^2_{\text{max}}$ for $B \to V$ ($B_{(q,s)} \to (K^*, \phi)$) FFs. Unquenched calculations are coming out with 2+1-flavors of dynamical fermions [46–48] in the narrow width approximation of the vector mesons. $B \to K$ FFs can be found in [49, 50] also using 2+1-flavor dynamical configurations.

4.2 Finite width effects

The vector meson decay via the strong force, e.g. $K^* \to K\pi$ and do therefore have a sizeable width and it is legitimate to ask how each formalism deals with this problem.

[3] Alternatively one may use the B-meson DA and an interpolating current for the K^*-meson e.g. [44] for a tree-level computation with therefore slightly larger uncertainties with results compatible with [10, 43].

For LCSR the answer is surprisingly pragmatic in that the formalism automatically adapts to the experimental handling of the vector meson resonance. In LCSR the vector meson are described by LCDAs which may schematically be written as

$$\langle K^*(p,\eta)|\bar{s}(x)\gamma_\mu\gamma_5 q(0)|0\rangle = m_{K^*} f_{K^*} p_\mu \int_0^1 du e^{up\cdot x}\phi_\parallel(u) + \text{higher twist}\,, \tag{12}$$

where it is assumed $p = m_{K^*}\eta$ (valid upon neglecting higher twist effects $O(x^2, m_K^*)$). The variable u is the momentum fraction of the s-quark in the infinite momentum frame. The decay constant f_{K^*} parametrises the leading conformal partial wave. Since the remaining part (higher Gegenbauer moments) contribute 10-15% only, the question of finite width effects is from the pragmatic viewpoint the same as to how well-defined f_{K^*} is. Whereas the latter can be computed from QCD sum rules or lattice module finite width effects, they can be extracted from experiment e.g. $\tau \to K^*\nu$ (see appendix C in Ref. [10] for a review). Consistency is then ensured by using the the same quantity in LCSR FFs prediction and an equivalent treatment of the $K*$-meson in $B \to (K\pi)_{l=1}\mu\mu$ by the experimentalist. In summary, consistency is achieved when the experimental projection of the $(K\pi)_{l=1}$-wave on the K^* is treated consistently across the experiments and the same f_{K^*} is used for the LCSR FF predictions. The transversal decay constant, $f_{K^*}^\perp$, is though not experimentally accessible and is preferably taken from the ratio $f_{K^*}/f_{K^*}^\perp$ which can be computed from QCD sum rules or lattice QCD. One expects would then expect finite width effects to drop out in this ratio which could be verified in the QCD sum rules approach or by extrapolating to lower quark masses in lattice QCD simulations. In conclusion this allows to bypass a first principle definition of the K^*-meson as a pole on the second sheet and the induced error can be seen as negligible compared to the remaining uncertainty.

A fully controlled lattice QCD computation of FFs involving a vector meson needs to include scattering states. This requires much more sophisticated and expensive calculations. In existing lattice calculations of the FFs, the threshold effects are assumed to be small in the narrow width approximation. Since ϕ is relatively narrow, one might expect this approximation is better than in the case of K^*. In $B \to D^*$ FFs heavy meson chiral perturbation theory predicts percent-level threshold effects [51, 52]. One might hope this is also true for lighter mesons. To fully quantify these effects, a systematic calculation should be performed. The Maiani-Testa no-go theorem [53] says there is no simple relation between correlators calculated in Euclidean space by lattice QCD and the transition matrix elements in Minkowski space when multiple hadrons are involved in the initial or final states. The first formalism to overcome this problem is the Lellouch-Lüscher method [54] which relates matrix elements of currents in finite volume to those in the infinite volume. Recent developments of this formalism and progresses on the lattice can be found in, for examples, Refs. [55–60]. Their implementations on B meson one to two matrix elements (e.g. $B \to K\pi$) may be expected in the future.

4.3 The use of the equations of motion (projection on B-meson ground state)

Both in LCSR and lattice the B-meson is described by an interpolating current and it is therefore a legitimate question of what the precision of the projection on the B-meson ground state is.[4] Below we argue that the EOM do improve the situation.

[4] In both cases this is in practice achieved by an exponential suppression of the higher states. If one was able to compute the correlation function exactly in Minkowski space then one could use the LSZ-formalism. Hence the method used can be seen as approximate methods to the latter.

The vector and tensor operators entering (11) are related by EOMs

$$\begin{aligned}\langle K^*|i\partial^\nu(\bar{s}i\sigma_{\mu\nu}b)|B\rangle &= -(m_s \pm m_b)\langle K^*|\bar{s}\gamma_\mu b|B\rangle + i\partial_\mu\langle K^*|(\bar{s}b)|B\rangle - 2\langle K^*|\bar{s}i\overleftarrow{D}_\mu\, b|B\rangle \\ \sim T_1(q^2) \quad &= \quad \sim \mathcal{V}_1(q^2) \quad + \quad \sim 0 \quad + \quad \sim \mathcal{D}_1(q^2) \end{aligned} \tag{13}$$

where the derivative term defines a new FF $\mathcal{D}_1(q^2)$ in analogy to $T_1(q^2)$. The EOM (13) are exact and have to be obeyed by any computation and can therefore be used as a non-trivial check for any computation per se. This has been done in [10] at the tree-level up to twist-4 and at the level of the Z-factors describing the renormalisation of the composite operators entering the EOM (13). Furthermore at the level of the effective Hamiltonian $\mathcal{D}_1(q^2)$ is redundant since the EOM have been applied. Eq. (13) therefore defines a relation between 3 FFs with one being redundant which does not appear to be helpful. The usefulness comes from the hierarchy $\mathcal{D}_1 \ll T_1, \mathcal{V}_1$ which constrains the vector in terms of the tensor FF [10, 61]. At the level of the actual computation this allows us to control the correlation of the continuum threshold parameters $s_0^{\mathcal{V}_1,T_1}$ which are a major source of uncertainty for individual FFs. The argument is that if those parameters were to differ by a sizeable amount for the vector and tensor FFs then the exactness of (13) would impose a huge shift for the corresponding parameters of the derivative FF corresponding to an absurd violation of semi-global quark hadron duality. Since $\mathcal{D}_1$ seems well-behaved in terms of convergence in the α_s- and the twist-expansion this possibility seems absurd and therefore supports the validity of the argument. It should be mentioned that the crucial hierarchy $\mathcal{D}_1 \ll T_1, \mathcal{V}_1$ can be traced back to the large energy limit [28]. For more details and a plot illustrating the validity of this argument over the q^2-range we refer the reader to references [10, 61] and Fig.1 of [10].

On the lattice the projection on the ground state would be perfect if one could go to infinite Euclidean time and if there was no noise. In practice simulation are done at a finite t-interval with some noise and this sets some limitations on the projection. On the positive side these aspects are improvable with more computer power. It is conceivable that the EOM can be used for the lattice in correlating the projection of FFs entering the same EOMs.

5 The relevance of charm contributions (R.Zwicky)

In FCNC processes of the type $B \to K^{(*)}\ell\ell$, the subprocesses $B \to K^{(*)}(\bar{c}c \to \gamma^* \to \ell\ell)$ is numerically relevant since it proceeds at tree-level. Hence the Wilson coefficients of operators of the form $O_{\text{charm}} \sim \bar{c}\gamma_\mu s_L \bar{b}\gamma^\mu c$ (combinations of $O_1^{(c)}$ and $O_2^{(c)}$ in standard terminology) in the effective Hamiltonian are sizeable. The other relevant aspect is that the four momentum invariant, $q^2 \in [4m_\ell^2, (m_B - m_{K^{(*)}})^2]$, of the lepton-pair takes on values in the region of charmonium resonances. Hence the process is sensitive to resonances, with photon quantum numbers $J^{PC} = 1^{--}$, and one can therefore not entirely rely on a partonic picture. It is customary to divide the q^2-spectrum into three regions (see Fig. 4). A region sufficiently well-below the first charmonium resonance at $q^2 = m_{J/\psi}^2 \simeq 9.6\,\text{GeV}^2$, the region of the two narrow charmonium resonances J/ψ and $\psi(2S)$ and the region of broad charmonium states starting around the $\bar{D}D$-threshold $q^2 \simeq 14\,\text{GeV}^2$. The crucial question is as to when and how partonic methods are applicable in the hadronic charmonium region. We discuss them below in the order of tractability in the partonic picture.

In the “below-charmonium region" partonic methods (i.e. α_s-expansion) are expected to be applicable. Since this is the region where the particles are fast in the B-rest frame, the physics can be described within a light-cone formalism. The order $O(\alpha_s^0)$ contribution is equivalent to naive factorisation (NF) which means that the amplitude factorises as follows

$$\mathcal{A}[B \to K^{(*)}\ell\ell]\Big|^{\text{NF}}_{O_{\text{charm}}} \sim h(q^2) F^{B\to K^{(*)}}(q^2)\,, \tag{14}$$

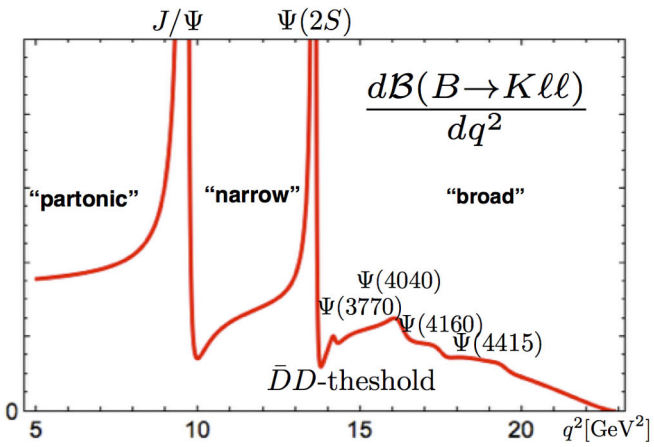

Figure 4. Illustration of the spectrum in q^2, the lepton pair invariant momentum, for the $B \to K\ell\ell$ branching fraction. The three region referred to in the text are the "below resonance region" (partonic, low-q^2), "narrow resonance region" and the "broad resonance region" (high-q^2).

where $F^{B\to K^{(*)}}(q^2)$ stands for the relevant form factor (FF) combination and $h(q^2)$ is the vacuum polarisation due to the charm-part of the electromagnetic current. At this formal level the light-cone aspect is only present in that the preferred method for evaluating the FFs are light-cone methods (see Sec. 4.1). Corrections of order $O(\alpha_s)$ are sizeable since the leading order contribution is colour-suppressed. Unfortunately the situation is not as favourable as at $O(\alpha_s^0)$ since the gluon exchanges limits factorisation making the problem more complex. Computations for vertex and hard spectator type corrections exist only in QCD factorisation relying on $1/m_b$-suppression [23, 24], with vertex corrections borrowed from inclusive computations [62]. These can be supplemented by contributions where a gluon interacts with the $K^{(*)}$ - and the B-meson [63, 64] (so far for $q^2 = 0$ only) and [41] respectively. In fact these contributions are related in that in an approach beyond factorisation (i.e. beyond the $1/m_b$-limit) one either works with a B- or $K^{(*)}$-LCDA. This is equivalent to a specific formulation of the light-cone OPE (i.e. twist-expansion, see Sec. 4.1 and footnote 3) within a LCSR-approach. A consistent treatment in α_s, beyond QCD factorisation, involves the computation of the vertex and hard spectator corrections as well as the emission of a gluon into the LCDA (higher twist) where the LCDA corresponds to either B- or $K^{(*)}$-meson. The vertex and hard spectator corrections have not been performed in either approach, partly, since the evaluation is difficult if one does not resort to approximations. The size of these contributions are therefore unknown beyond the heavy quark limit. A completion of this program is desirable as will become clear further below.

The "broad charmonium region" (see Fig. 4 on the right) is characterised by a considerable interference of the short-distance and charmonium long-distance part. The charmonium resonances $\psi(3770)$, $\psi(4040)$, $\psi(4160)$ and $\psi(4415)$ are broad because they can decay via the strong force into $\bar{D}D$-states. The resonances are necessarily accompanied by a continuum of $\bar{D}D$-states as is the case

in $e^+e^- \to hadrons$ [38]. A sketch of a realistic parametrisation is given by [5]

$$\mathcal{A}[B \to K^{(*)}\ell\ell]\Big|_{O_{\rm charm}} \simeq \sum_{\psi=J/\psi,\psi(2S),\psi(3770),..} \frac{r_\psi}{q^2 - m_\psi^2 + i m_\psi \Gamma_\psi} + f_{\bar{c}c}(q^2)\,, \tag{15}$$

where the residues r_ψ and the non-resonant $\bar{c}c$-continuum function $f_{\bar{c}c}$ are the unknowns which usually have to be determined experimentally. For $e^+e^- \to hadrons$, which effectively corresponds to NF (14), $r_\psi^{\rm NF} \sim \Gamma(\psi \to \ell\ell) F^{B\to K^{(*)}}(m_\psi^2) > 0$ and $f_{\bar{c}c}^{\rm NF}(q^2)$ ($\mathrm{Im}[f_{\bar{c}c}^{\rm NF}(q^2)] > 0$) for which successful parametrisations are easily found via dispersion relations [38, 65]. Going beyond factorisation involves determining the factors

$$\eta_\psi \equiv |\eta_\psi| e^{i\delta_\psi} = \frac{r_\psi}{r_\psi^{\rm NF}}\,, \qquad f_{\bar{c}c}(q^2)\,, \tag{16}$$

and the continuum function $f_{\bar{c}c}(q^2)$. The strong-phase δ_ψ is defined relative to the the FF contribution. The determination of $f_{\bar{c}c}(q^2)$ is a difficult task since the q^2-dependence could be similar to the one of the short distance contributions. The shape of the resonances is very distinct (e.g Fig. 4) and can therefore be fitted. This has been done in [38] using the LHCb-data [8]. A surprisingly good fit is obtained by $\eta_{\tilde{\psi}} \simeq -2.55$ with $\tilde{\psi}$ in $\{\psi(3770), \psi(4040), \psi(4160), \psi(4415)\}$.[6] One concludes that NF is badly broken and that the charm might impact on the low q^2-spectrum [38]. Note that even in the narrow width approximation the non-local part of the resonances (15) only decays as $1/q^2$ away from its centre.

These results bring the focus to the "narrow charmonium region". Whereas the absolute values $|\eta_{J/\psi}| \simeq 1.4$ and $|\eta_{\psi(2S)}| \simeq 1.8$ are known from the decay rates $\Gamma(B \to K^{(*)}\psi)$ the phases $\delta_{J/\psi,\psi(2S)}$ are not known. The need to extract the latter from experiment has been emphasised and suggested in [38] and recently been performed by the LHCb collaboration [22]. Unfortunately, so far, the solutions show a four-fold ambiguity $(\delta_{J/\psi}|\delta_{\psi(2S)}) \simeq (0, \pi|0, \pi)$. Whereas this is an important result one would hope that this ambiguity can be resolved with more data.

After this excursion let us discuss the practicalities for the low-q^2 ("below resonance region") and high-q^2 ("broad resonance region") regions where phenomenologists and experimentalists compare predictions to measurements in the hope of seeing physics beyond the Standard Model. It would be desirable to obtain a coherent picture of the partonic and hadronic description in both of these regions in order to validate the approaches. Both cases need more work. At low-q^2, as previously discussed, the partonic contributions are not very complete. For example, the sizeable vertex corrections of the charm loop are not known beyond the $1/m_b$-limit and one might therefore wonder about the size of the $1/m_b$-corrections. Generally the size of $1/m_b$-corrections are hard to predict, for FFs they are 10%, for the decay constant f_B 30% whereas for the O_8-matrix elements (chromomagnetic operator) they are 50% [66]. As for the hadronic data further work is needed in order to determine the strong phases $\delta_{J/\psi,\psi(2S)}$ as well as the continuum function $f_{\bar{c}c}(q^2)$. Before moving on it should be mentioned that the hadronic fits should and will be extended from $B \to K\ell\ell$ to $B \to K^*\ell\ell$ by the LHCb-collaboration. In the high-q^2 region a partonic picture has been advocated, known as the high-q^2 OPE, where one resorts to an expansion in $1/m_b$ and $1/\sqrt{q^2}$ supplemented by charm-contributions [36, 37]. The initial idea was to to include charm contributions in an α_s-expansion, relying on cancellations when averaged

[5] More realistic parameterisation are different in two aspects. Firstly, they only parameterise the discontinuity and the remaining part is obtained by a dispersion relation e.g. $e^+e^- \to hadrons$ [65] and $B \to K\ell\ell$ [38]. Second they include energy dependent width effects and interferences of the overlapping broad resonances. This has been successfully done in $e^+e^- \to hadrons$ [65] and adapted to $B \to K\mu\mu$ in [38]. The inclusion of interference effects reduces the χ^2/d.o.f. from $\simeq 1.4$ to $\simeq 1$. Crucially the degree of model dependence is justified by the success of the fit.

[6] These findings have recently been confirmed by the LHCb collaboration [22].

over large enough bins.[7] As an estimate of these quark-hadron duality violations NF was taken as a guidance [37] yielding a 2% effect. One is then faced with the fact that the actual data [8] show much larger effects in the 10%-region [38].[8] Hence replacing the partonic charm contribution with a hadronic dispersion relation (15) for the high-q^2 OPE might be a viable alternative . The bottleneck is though the determination of the the continuum function $f_{\bar{c}c}(q^2)$. A promising direction could be the experimental investigation of the $B \to \bar{D}DK^{(*)}$ modes.

In summary clarifying the role of the charm will remain an outstanding task before angular anomalies of the $B \to K^*\ell\ell$-type, not related to lepton flavour violation, can be considered to be physics beyond the Standard Model. Future investigations are needed and are currently pursued by experimentalists and theorists.

6 Global fits (L. Hofer)

As reported in Sec. 2, experimental results on $B \to K^*\mu^+\mu^-$, $B_s \to \phi\mu^+\mu^-$ and $R_K = Br(B \to K\mu^+\mu^-)/Br(B \to Ke^+e^-)$ show deviations from the SM at the $2-3\sigma$ level. Although none of these tensions is yet significant on its own, the situation is quite intriguing as the affected decays are all mediated by the same quark-level transition $b \to s\ell^+\ell^-$ and thus probe the same high-scale physics. A correlated analysis of these channels can shed light on the question whether a universal new-physics contribution to $b \to s\ell^+\ell^-$ can simultaneously alleviate the various tensions and lead to a significantly improved global description of the data.

At the energy scale of the $B_{(s)}$ decays, any potential high-scale new physics mediating $b \to s\ell^+\ell^-$ transitions can be encoded into the effective couplings $C^{(\prime)}_{7,9,10}$ multiplying the operators

$$\begin{aligned} O^{(\prime)}_9 &= \frac{\alpha}{4\pi}[\bar{s}\gamma^\mu P_{L(R)}b][\bar{\mu}\gamma_\mu\mu], \qquad O^{(\prime)}_{10} = \frac{\alpha}{4\pi}[\bar{s}\gamma^\mu P_{L(R)}b][\bar{\mu}\gamma_\mu\gamma_5\mu], \\ O^{(\prime)}_7 &= \frac{\alpha}{4\pi}m_b[\bar{s}\sigma_{\mu\nu}P_{R(L)}b]F^{\mu\nu}, \end{aligned} \tag{17}$$

where $P_{L,R} = (1\mp\gamma_5)/2$ and m_b denotes the b quark mass. Whereas the above-mentioned semi-leptonic decays are sensitive to the full set $C^{(\prime)}_{7,9,10}$ of effective couplings, the decay $B_s \to \ell^+\ell^-$ only probes $C^{(\prime)}_{10}$ and $B \to X_s\gamma$, $B \to K^*\gamma$ set constraints on $C^{(\prime)}_7$. Note that additional scalar or pseudoscalar couplings $C_{S,S',P,P'}$ cannot address the tensions in exclusive semi-leptonic B decays since their contributions are suppressed by small lepton masses.

Various groups have performed fits of the couplings $C^{(\prime)}_{7,9,10}$ to the data [9, 69–72]. The obtained results are in mutual agreement with each other and confirm the observation, pointed out for the first time in Ref. [70] on the basis of the 2013 data, that a large negative new-physics contribution C_9 yields a fairly good description of the data. This is illustrated in Tab. 1, where selected results from Ref. [69] for one-parameter fits of the couplings $C^{(\prime)}_{7,9,10}$ are displayed. Apart from the best-fit point together with the 1σ region, the tables feature the SM-pull of the respective new-physics scenarios. This number quantifies by how many sigmas the best fit point is preferred over the SM point $\{C^{\rm NP}_i\} = 0$ and

[7] The gateway to quark-hadron duality are dispersion relations valid at the level of amplitudes. Averaging at the decay rate level is only valid if the rate can be written as an amplitude which is the case for inclusive modes such as $e^+e^- \to hadrons$ and not the case for $B \to K^{(*)}\ell\ell$. Averaging over the entire $B \to K^{(*)}\ell\ell$-rate, which includes the narrow resonances, fails by several orders of magnitudes as discussed and clarified in [67].

[8] For angular observable observables the situation is more favourable in two aspects partly at the cost of sensitivity to new physics. Firstly, in the limit of no right-handed currents and constant $\eta_{\tilde{\psi}}$ resonance effects drop out in a few angular observables [61]. Second at the kinematic endpoint $q^2 = (m_B - m_{K^{(*)}})^2$ the observables approach exact values based on Lorentz-covariance only (i.e. valid in any model and approximation which respects Lorentz invariance) and show a certain degree of universality near the endpoint region [68].

Coefficient	Best fit	1σ	Pull_{SM}
C_7^{NP}	-0.02	$[-0.04, -0.00]$	1.2
$\mathbf{C_9^{NP}}$	$\mathbf{-1.09}$	$[-1.29, -0.87]$	**4.5**
C_{10}^{NP}	0.56	$[0.32, 0.81]$	2.5
$C_7'^{\text{NP}}$	0.02	$[-0.01, 0.04]$	0.6
$C_9'^{\text{NP}}$	0.46	$[0.18, 0.74]$	1.7
$C_{10}'^{\text{NP}}$	-0.25	$[-0.44, -0.06]$	1.3
$C_9^{\text{NP}} = C_{10}^{\text{NP}}$	-0.22	$[-0.40, -0.02]$	1.1
$\mathbf{C_9^{NP} = -C_{10}^{NP}}$	$\mathbf{-0.68}$	$[-0.85, -0.50]$	**4.2**
$\mathbf{C_9^{NP} = -C_9'^{NP}}$	$\mathbf{-1.06}$	$[-1.25, -0.85]$	**4.8**

Fit	$C_{9\,\text{Bestfit}}^{\text{NP}}$	1σ	Pull_{SM}
All $b \to s\mu\mu$	-1.09	$[-1.29, -0.87]$	4.5
$b \to s\mu\mu$ without $q^2 \in [6, 8]$	-0.99	$[-1.23, -0.75]$	3.8
$b \to s\mu\mu$ large recoil	-1.30	$[-1.57, -1.02]$	4.0
$b \to s\mu\mu$ low recoil	-0.93	$[-1.23, -0.61]$	2.8
Only $B \to K\mu\mu$	-0.85	$[-1.67, -0.20]$	1.4
Only $B \to K^*\mu\mu$	-1.05	$[-1.27, -0.80]$	3.7
Only $B_s \to \phi\mu\mu$	-1.98	$[-2.84, -1.29]$	3.5

Table 1. Left: best-fit point, 1σ region and SM-pull for 1-parameter fits allowing new physics only in one of the couplings $C_{7,9,10}^{(\prime)}$. Right: fits of a new-physics contribution to the effective coupling C_9 using different subsets of the experimental data as input. Results are taken from Ref. [69]

thus measures the capacity of the respective scenario to accommodate the data. The table on the left demonstrates that a large negative new-physics contribution C_9 is indeed mandatory to significantly improve the quality of the fit compared to the SM. It is particularly encouraging that the individual channels tend to prefer similar values for C_9, as shown in the table on the right.

The results of the fit are quite robust with respect to the hadronic input and the employed methodology. This can be seen from the good agreement between the results of the analyses AS [9] and DHMV [69] which use approaches that are complementary in many respects:

- AS choose the observables S_i as input for the fit to the angular distributions of $B \to K^*\ell^+\ell^-$ and $B_s \to \phi\ell^+\ell^-$ and restrict their fits in the region of large K^*-recoil to squared invariant dilepton masses $q^2 \in [1, 6]\,\text{GeV}^2$. DHMV, on the other hand, choose the observables $P_i^{(\prime)}$, which feature a reduced sensitivity to the non-perturbative form factors, and include all bins up to $q^2 = 8\,\text{GeV}^2$.
- AS use LCSR form factors from Ref. [10], while DHMV mainly resort to the LCSR form factors from Ref. [41].
- In the analysis of AS, correlations among the form factors are implemented on the basis of the LCSR calculation [10], whereas in the analysis of DHMV they are assessed from large-recoil symmetries supplemented by a sophisticated estimate of symmetry-breaking corrections of order $O(\Lambda/m_b)$. The pros and cons of these two methods complement each other: The first approach provides a more complete access of correlations at the price of a dependence on and the limitation to one particular LCSR calculation [10] and its intrinsic model-assumptions. The second approach determines the correlations in a model-independent way from first principles but needs to rely on an estimate of subleading non-perturbative Λ/m_b corrections.

The measurement of $R_K \neq 1$ hints at a possible violation of lepton-flavour universality (LFUV) and suggests a situation where the muon- and the electron-components of the operators $C_{9,10}^{(\prime)}$ receive independent new-physics contributions $C_{i\,\mu}^{\text{NP}}$ and $C_{i\,e}^{\text{NP}}$, respectively. In Fig. 5 on the left we display the result for the two-parameter fit to the coefficients $C_{9\,\mu}^{\text{NP}}$ and $C_{9\,e}^{\text{NP}}$. The plot is taken from Ref. [69], similar results are obtained in Refs. [9, 72]. The fit prefers an electron-phobic scenario with new physics coupling to $\mu^+\mu^-$ but not to e^+e^-. Under this hypothesis, that should be tested by measuring R_{K^*} and R_ϕ, the SM-pull increases by $\sim 0.5\sigma$ compared to the value in Tab. 1 for the lepton-flavour universal scenario, except for the scenario with $C_9^{\text{NP}} = -C_9'^{\text{NP}}$ where the value remains unchanged due to the absence of any contribution to R_K.

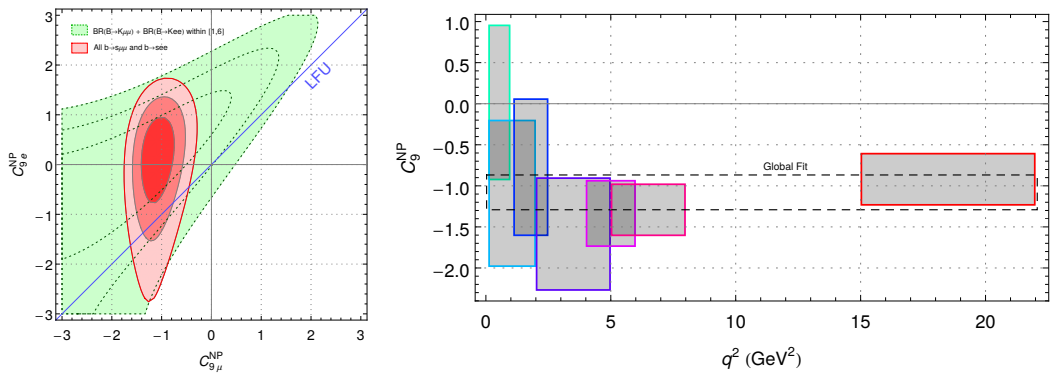

Figure 5. Left: Fit allowing for LFUV by means of independent coefficients $C_{9\,\mu}^{\rm NP}$ and $C_{9\,e}^{\rm NP}$. Right: Bin-by-bin fit of the one-parameter scenario with a single coefficient $C_9^{\rm NP}$. Reproduced from Ref. [69].

The fact that it is primarily the variation of the coefficient C_9 which is responsible for solving the anomalies unfortunately spoils an unambigous interpretation of the fit results in terms of new physics. The reason is that precisely this effective coupling can be mimicked by non-perturbative charm loops, as discussed in Sec. 5. However, whereas these non-local effects are expected to introduce a non-trivial dependence on the squared invariant mass q^2 of the lepton pair, a high-scale new-physics solution would necessarily generated a q^2 independent $C_9^{\rm NP}$. A promising strategy to resolve the nature of potential non-standard contribution to the effective coupling C_9 thus consists in the investigation of its q^2 dependence. To this end, two different methods have been pursued so far: In Ref. [73], the authors performed a bin-by-bin fit of C_9 to check whether results in different bins were consistent with each other under the hypothesis of a q^2-independent C_9. Their conclusion, which was later confirmed also in Ref. [69] with the plot shown in Fig. 5 on the right, was that there is no indication for a q^2-dependence, though the situation is not conclusive due to the large uncertainties in the single bins.

An alternative strategy to address this question has been followed recently in Refs. [42, 74] where a direct fit of the q^2-dependent charm contribution $C_9^{c\bar{c}\,i}(q^2)$ to the data on $B \to K^*\mu^+\mu^-$ (at low q^2) has been performed under the hypothesis of the absence of new physics. The results are in agreement with the findings from Fig. 5: in Ref. [74] it was shown that the inclusion of additional terms parametrising a non-trivial q^2-dependence does not improve the quality of the fit. On the other hand, current precision of the experimental data does not allow to exclude non-zero values for these terms.

7 BSM interpretation (L. Hofer)

As we have seen in the previous section, the observed anomalies in $b \to s\ell^+\ell^-$ decays show a coherent picture and allow for a solution at the level of the effective Hamiltonian by NP contributions to the operators $O_{9,10}^{(\prime)}$. At tree level, contributions to these operators can be mediated by exchange of a heavy neutral vector-boson Z' (e.g. [70, 75–84]), or by scalar or vector lepto-quarks (e.g. [85–90]). At one loop, they can be generated by box diagrams involving new particles (e.g. [91–93]) or by Z' penguins (e.g. [94]). The step beyond the model-independent analysis allows to attempt a common explanation of the $b \to s\ell^+\ell^-$ anomalies with other tensions in flavour data, like $R_{D^{(*)}}$ or the long-standing anomaly in the anomalous magnetic moment of the muon. It further permits to study the viability of the various

model classes in the light of constraints from other flavour observables and from direct searches. In the following, we will briefly summarize typical Z' and lepto-quark scenarios, and discuss bounds from $B_s - \overline{B}_s$ mixing and direct searches.

7.1 Z' models

The interaction of a generic Z' boson with the SM fermions is described by the Lagrangian

$$\mathcal{L}_{Z'} = \sum_{ff'} \Gamma^L_{ff'} \bar{f} \gamma^\mu P_L f' Z'_\mu + \Gamma^R_{f,f'} \bar{f} \gamma^\mu P_R f' Z'_\mu + \text{h.}c., \tag{18}$$

where the sum is over fermions f, f' with equal electric charges. The exact form of the couplings $\Gamma^{L,R}_{ij}$ depends on the $U(1)'$ charges assigned to the SM fermions and on a potential embedding of the Z' in a more fundamental theory. Note, however, that $SU(2)_L$ invariance implies the model-idependent relations $\Gamma^L_{uu'} = V_{ud} \Gamma^L_{dd'} V^\dagger_{u'd'}$ and $\Gamma^L_{\ell\ell'} = \Gamma^L_{\nu_\ell \nu_{\ell'}}$ (with V denoting the CKM matrix).

The Wilson coefficients $C^{(\prime)}_{9,10}$ are generated by tree-level Z' exchange involving products of couplings $\Gamma^{L,R}_{bq} \Gamma^{L,R}_{\ell\ell}$. Since only three out of these four products are independent, the relation $C_9 \cdot C'_{10} = C'_9 \cdot C_{10}$ is fulfilled in models with a single Z' boson. In order to generate a non-vanishing coupling $C_{9\mu}$, mandatory for a solution of the $b \to s\ell^+\ell^-$ anomalies, the couplings Γ^L_{bs} and $\Gamma^L_{\mu\mu} + \Gamma^R_{\mu\mu}$ need to have non-vanishing values.

The most popular class of Z' models is based on gauging $L_\tau - L_\mu$ lepton number [78, 81, 82, 95, 96]. This pattern of $U(1)'$ charges avoids anomalies and is well-suited to generate the measured PMNS matrix. The vanishing coupling of the Z' to electrons allows to explain LFUV in R_K and helps to avoid LEP bounds on the Z' mass $M_{Z'}$. The symmetry can be extended to the quark sector with a flavour non-universal assignment of $U(1)'$ charges that induces the off-diagonal couplings $\Gamma^{L,R}_{bs}$ (e.g. [79, 82]). An alternative mechanism to generate the couplings $\Gamma^{L,R}_{bs}$ consists in the introduction of additional vector-like quarks that are charged under the $U(1)'$ symmetry and that generate an effective bsZ' coupling via their mixing with the SM fermions [78, 81, 95, 97].

Several Z' scenarios have been proposed that are capable of solving not only the $b \to s\ell^+\ell^-$ anomalies but at the same time also other tensions in the data. Embedding the Z' in a $SU(2)'$ gauge model allows to address the anomalies in $R_{D^{(*)}}$ with a tree-level contribution to $b \to c\ell^-\bar{\nu}$ mediated by the W'-boson (e.g. [83, 98]). It is also possible to solve the anomaly in $(g-2)_\mu$ in a Z' scenario, provided the Z' coupling to muons is generated at the loop-level so that both the NP contributions to $b \to s\ell^+\ell^-$ and $(g-2)_\mu$ are loop-suppressed [94].

7.2 Lepto-quark models

Lepto-quarks are new particles Δ_k beyond the SM that couple leptons to quarks via vertices $\ell_i q_j \Delta_k$. Different lepto-quark models can be classified according to the spin of the lepto-quarks and their quantum numbers with respect to the SM gauge groups. Since the $\ell_i q_j \Delta_k$ couplings violate lepton-flavour, lepto-quark models are excellent candidates to explain LFUV observables like R_K and $R_{D^{(*)}}$. Indeed, various representations of lepto-quarks have been studied with respect to their capability of accommodating the measured values of R_K and $R_{D^{(*)}}$ by tree-level lepto-quark contributions [85–90]. In Ref. [92] it was further proposed that an $SU(2)_L$ singlet scalar lepto-quark could explain $R_{D^{(*)}}$ by a tree-level and R_K by a loop contribution. This possibility was later shown in Ref. [99] to be challenged by other flavour data.

7.3 Constraints from $B_s - \overline{B}_s$ mixing and direct searches

A NP model generating $b \to s\ell^+\ell^-$ necessarily also contributes to $B_s - \bar{B}_s$ mixing. In lepto-quark models, $b \to s\ell^+\ell^-$ is typically mediated at tree level, while $B_s - \bar{B}_s$ mixing contributions are loop-suppressed and thus do not pose relevant contraints. In Z' models, on the other hand, both processes are usually generated by tree-level exchange of the Z' boson. The constraint on $|\Gamma^{L,R}_{bs}|/M_{Z'}$ from $B_s - \bar{B}_s$ mixing then imposes a lower limit $|\Gamma^{L,R}_{\mu\mu}|/M_{Z'} \gtrsim 0.3/(1\,\text{TeV})$ that needs to be reached for a solution of the $b \to s\mu^+\mu^-$ anomalies. In models with box contributions to both $b \to s\ell^+\ell^-$ and $B_s - \overline{B}_s$ mixing, the analogous constraint is more severe due to the loop suppression: $|\Gamma_\mu|/\sqrt{M_\Phi} \gtrsim 3/\sqrt{1\,\text{TeV}}$ where M_Φ denotes the mass scale of the new particles in the box and Γ_μ their coupling strength to the muon. It was shown in Ref. [93] that this bound can be relaxed in a scenario with Majorana fermions in the box where the additional crossed boxes lead to a negative interference in $B_s - \overline{B}_s$ mixing.

Bounds from direct searches can be avoided to a large extent if the new physics couples only to the second and third fermion generation, in line with LFUV in R_K and $R_{D^{(*)}}$. Collider signals are then limited to more complex final state, like e.g. $pp \to 4\mu$ probing the muon-coupling of a possible Z' boson, or to suppressed production channels, like e.g. $b\bar{s} \to \mu^+\mu^-$. However, it was found [100] very recently that the data from Atlas/CMS already now heavily constrains Z' and lepto-quark scenarios even in the $b\bar{b} \to \tau^+\tau^-$ channel: a solution of $R_{D^{(*)}}$ by SU(2)$'$ gauge bosons W'/Z' is restricted to masses $M_{Z'} \lesssim 500\,\text{GeV}$, and a solution via vector lepto-quarks is about to be excluded. The interplay with high-p_T searches will thus definitely play a crucial role in the quest for an explanation of the flavour anomalies.

8 Summary

The discovery of the leptonic decay $B^0_s \to \mu^+\mu^-$ by the CMS and LHCb collaborations was a major breakthrough of precision flavour physics with data from Run 1 of the Large Hadron Collider. Since then, several anomalies have emerged in semileptonic decays. These indicate a potential violation of lepton universality in the decays $B \to K^{(*)}\mu^+\mu^-$ and $B \to K^{(*)}e^+e^-$ with a statistical significance of 2.6σ. In the angular analysis of $B \to K^*\mu^+\mu^-$ decays, tensions with the SM are seen in the longitudinal polarisation of the K^* and the angular observable P'_5. The largest discrepancy with more than 3σ is seen in the differential branching fraction of the decay $B^0_s \to \phi\mu^+\mu^-$.

The dynamics of $B \to K^*\mu^+\mu^-$ decays can be described by a set of helicity amplitudes, which, in the effective Hamiltonian formalism, split into Wilson coefficients and matrix elements of local operators. Deviations in the Wilson coefficient C_9, which is sensitive to new physics as well as long-distance QCD, can explain the experimental data. The most sensitive observables to C_9 are the q^2 dependence of the forward-backward asymmetry and the angular observable P'_5. These observables have been constructed such that they exhibit a reduced sensitivity to hadronic form factors, though a remnant dependence at order Λ/m_b cannot be avoided and its impact cannot be predicted in the HQET framework. A combination of light-cone sum rule calculations with more precise measurements may be able to address this issue.

In light-cone sum rule computation finite width effects can effectively be bypassed if the vector mesons are treated consistently in all experiments, which includes the ones from where input is taken for form factor calculations as well as the one were the form factor computations are used. Whereas current lattice QCD studies do not include finite width effects, recent developments indicate that this may change in the foreseeable future. The use of equation of motion reduces the uncertainty of the projection on the B-meson state for ratios of form factors in light-cone sum rules. It is conceivable that the use of equation of motion might help to further improve lattice QCD computation as well.

The main focus of recent discussions have been the so-called charm contributions, which describe the sub-process $B \to K^{(*)}(\bar{c}c \to g_A^* \to \ell\ell)$. The data are typically studied in different regions of q^2: the 'partonic' well below the J/ψ resonance, the 'narrow' between the J/ψ and $\psi(2S)$ resonances, and the 'broad' in the high-q^2 region that is dominated by broad charmonium resonances. Ideally, a coherent description of the low and high q^2 regions should be obtained. Overcoming these challenges requires close collaboration of experimentalists and theorists to pursue new approaches such as a detailed study of the decays $B \to \bar{D}DK^{(*)}$.

Global fits aim to exploit a maximum of information of the range of observables in the framework of an effective theory. This allows the splitting of Wilson coefficients in a SM part and a component to encapsulate effects beyond the SM. Most fits favour a non-SM value of the coefficient C_9 of about -1 with the pull of the SM scenario exceeding 4σ in several cases. As contributions from high scales beyond the SM create q^2-independent effects, it is instructive to perform fits is several regions of q^2 and test for q^2-dependent effects that would indicate low-scale SM effects. At the current level of precision these tests are consistent with a q^2-independent shift of C_9.

Possible explanations involving particles beyond the SM exist in the form of lepto-quarks or Z' bosons, typically mediating the $b \to s\ell^+\ell^-$ transitions through tree-level exchange. In addition, these SM extensions have the potential to simultaneously accommodate other anomalies like $R_{D^{(*)}}$ or the anomalous magnetic moment of the muon. Direct searches pose tight constraints on some of these models and are expected to either probe or severely challenge them in the near future.

The number of flavour anomalies that appear to fit a common picture is intriguing. The analysis of data taken during the ongoing Run 2 of the LHC will yield powerful new insight both into the observables of interest and into new strategies to control uncertainties. The interpretation of these results requires close collaboration with theory, where advances are required in several areas for which promising strategies exist.

References

[1] H. Albrecht et al. (ARGUS collaboration), Phys. Lett. **B192**, 245 (1987), [,51(1987)]
[2] C. Bobeth, M. Gorbahn, T. Hermann, M. Misiak, E. Stamou, M. Steinhauser, Phys. Rev. Lett. **112**, 101801 (2014), 1311.0903
[3] V. Khachatryan et al. (CMS and LHCb collaborations), Nature **522**, 68 (2015), 1411.4413
[4] M. Aaboud et al. (ATLAS collaboration), Eur. Phys. J. **C76**, 513 (2016), 1604.04263
[5] R. Aaij et al. (LHCb collaboration), JHEP **06**, 133 (2014), 1403.8044
[6] R. Aaij et al. (LHCb collaboration), JHEP **09**, 179 (2015), 1506.08777
[7] V. Khachatryan et al. (CMS collaboration), Phys. Lett. **B753**, 424 (2016), 1507.08126
[8] R. Aaij et al. (LHCb collaboration), Phys. Rev. Lett. **111**, 112003 (2013), 1307.7595
[9] W. Altmannshofer, D.M. Straub, Eur. Phys. J. **C75**, 382 (2015), 1411.3161
[10] A. Bharucha, D.M. Straub, R. Zwicky, JHEP **08**, 098 (2016), 1503.05534
[11] R.R. Horgan, Z. Liu, S. Meinel, M. Wingate, Phys. Rev. Lett. **112**, 212003 (2014), 1310.3887
[12] R. Aaij et al. (LHCb collaboration), Phys. Rev. Lett. **113**, 151601 (2014), 1406.6482
[13] P. Golonka, Z. Was, Eur.Phys.J. **C45**, 97 (2006), hep-ph/0506026
[14] S. Agostinelli et al. (GEANT4 collaboration), Nucl. Instrum. Meth. **A506**, 250 (2003)
[15] J.P. Lees et al. (BaBar collaboration), Phys. Rev. **D93**, 052015 (2016), 1508.07960
[16] J.T. Wei et al. (Belle collaboration), Phys. Rev. Lett. **103**, 171801 (2009), 0904.0770
[17] T. Aaltonen et al. (CDF collaboration), Phys. Rev. Lett. **108**, 081807 (2012), 1108.0695
[18] R. Aaij et al. (LHCb collaboration), JHEP **02**, 104 (2016), 1512.04442

[19] A. Abdesselam et al. (Belle collaboration) (2016), BELLE-CONF-1603, 1604.04042
[20] S. Descotes-Genon, L. Hofer, J. Matias, J. Virto, JHEP **12**, 125 (2014), 1407.8526
[21] S. Jäger, J. Martin Camalich, JHEP **05**, 043 (2013), 1212.2263
[22] R. Aaij et al. (LHCb collaboration) (2016), 1612.06764
[23] M. Beneke, T. Feldmann, D. Seidel, Nucl. Phys. **B612**, 25 (2001), hep-ph/0106067
[24] S.W. Bosch, G. Buchalla, Nucl. Phys. **B621**, 459 (2002), hep-ph/0106081
[25] M. Beneke, T. Feldmann, D. Seidel, Eur. Phys. J. **C41**, 173 (2005), hep-ph/0412400
[26] T. Becher, R.J. Hill, M. Neubert, Phys. Rev. **D72**, 094017 (2005), hep-ph/0503263
[27] W. Altmannshofer, P. Ball, A. Bharucha, A.J. Buras, D.M. Straub, M. Wick, JHEP **01**, 019 (2009), 0811.1214
[28] J. Charles, A. Le Yaouanc, L. Oliver, O. Pene, J.C. Raynal, Phys. Rev. **D60**, 014001 (1999), hep-ph/9812358
[29] M. Beneke, T. Feldmann, Nucl. Phys. **B592**, 3 (2001), hep-ph/0008255
[30] M. Beneke, T. Feldmann, Nucl. Phys. **B685**, 249 (2004), hep-ph/0311335
[31] M. Beneke, Y. Kiyo, D.s. Yang, Nucl. Phys. **B692**, 232 (2004), hep-ph/0402241
[32] R.J. Hill, T. Becher, S.J. Lee, M. Neubert, JHEP **07**, 081 (2004), hep-ph/0404217
[33] T. Becher, R.J. Hill, JHEP **10**, 055 (2004), hep-ph/0408344
[34] M. Beneke, D. Yang, Nucl. Phys. **B736**, 34 (2006), hep-ph/0508250
[35] G. Buchalla, G. Isidori, Nucl. Phys. **B525**, 333 (1998), hep-ph/9801456
[36] B. Grinstein, D. Pirjol, Phys. Rev. **D70**, 114005 (2004), hep-ph/0404250
[37] M. Beylich, G. Buchalla, T. Feldmann, Eur. Phys. J. **C71**, 1635 (2011), 1101.5118
[38] J. Lyon, R. Zwicky (2014), 1406.0566
[39] J. Matias, F. Mescia, M. Ramon, J. Virto, JHEP **04**, 104 (2012), 1202.4266
[40] S. Jäger, J. Martin Camalich, Phys. Rev. **D93**, 014028 (2016), 1412.3183
[41] A. Khodjamirian, T. Mannel, A.A. Pivovarov, Y.M. Wang, JHEP **09**, 089 (2010), 1006.4945
[42] M. Ciuchini, M. Fedele, E. Franco, S. Mishima, A. Paul, L. Silvestrini, M. Valli, JHEP **06**, 116 (2016), 1512.07157
[43] P. Ball, R. Zwicky, Phys. Rev. **D71**, 014029 (2005), hep-ph/0412079
[44] A. Khodjamirian, T. Mannel, N. Offen, Phys. Rev. **D75**, 054013 (2007), hep-ph/0611193
[45] P. Ball, R. Zwicky, Phys. Rev. **D71**, 014015 (2005), hep-ph/0406232
[46] R.R. Horgan, Z. Liu, S. Meinel, M. Wingate, Phys. Rev. **D89**, 094501 (2014), 1310.3722
[47] R.R. Horgan, Z. Liu, S. Meinel, M. Wingate, PoS **LATTICE2014**, 372 (2015), 1501.00367
[48] J. Flynn, T. Izubuchi, A. Juttner, T. Kawanai, C. Lehner, E. Lizarazo, A. Soni, J.T. Tsang, O. Witzel, *Form factors for semi-leptonic B decays*, in *34th International Symposium on Lattice Field Theory (Lattice 2016)* (2016), 1612.05112, https://inspirehep.net/record/1504065/files/arXiv:1612.05112.pdf
[49] C. Bouchard, G.P. Lepage, C. Monahan, H. Na, J. Shigemitsu (HPQCD collaboration), Phys. Rev. **D88**, 054509 (2013), [Erratum: Phys. Rev.D88,no.7,079901(2013)], 1306.2384
[50] J.A. Bailey et al., Phys. Rev. **D93**, 025026 (2016), 1509.06235
[51] L. Randall, M.B. Wise, Phys. Lett. **B303**, 135 (1993), hep-ph/9212315
[52] S. Hashimoto, A.S. Kronfeld, P.B. Mackenzie, S.M. Ryan, J.N. Simone, Phys. Rev. **D66**, 014503 (2002), hep-ph/0110253
[53] L. Maiani, M. Testa, Phys. Lett. **B245**, 585 (1990)
[54] L. Lellouch, M. Luscher, Commun. Math. Phys. **219**, 31 (2001), hep-lat/0003023

[55] M.T. Hansen, S.R. Sharpe, Phys. Rev. **D86**, 016007 (2012), 1204.0826
[56] R.A. Briceño, M.T. Hansen, A. Walker-Loud, Phys. Rev. **D91**, 034501 (2015), 1406.5965
[57] J.J. Dudek, R.G. Edwards, C.E. Thomas, D.J. Wilson (Hadron Spectrum collaboration), Phys. Rev. Lett. **113**, 182001 (2014), 1406.4158
[58] S. Prelovsek, L. Leskovec, C.B. Lang, D. Mohler, Phys. Rev. **D88**, 054508 (2013), 1307.0736
[59] D.J. Wilson, J.J. Dudek, R.G. Edwards, C.E. Thomas, Phys. Rev. **D91**, 054008 (2015), 1411.2004
[60] A. Agadjanov, V. Bernard, U.G. Meißner, A. Rusetsky, Nucl. Phys. **B910**, 387 (2016), 1605.03386
[61] C. Hambrock, G. Hiller, S. Schacht, R. Zwicky, Phys. Rev. **D89**, 074014 (2014), 1308.4379
[62] H.H. Asatrian, H.M. Asatrian, C. Greub, M. Walker, Phys. Lett. **B507**, 162 (2001), hep-ph/0103087
[63] P. Ball, G.W. Jones, R. Zwicky, Phys. Rev. **D75**, 054004 (2007), hep-ph/0612081
[64] F. Muheim, Y. Xie, R. Zwicky, Phys. Lett. **B664**, 174 (2008), 0802.0876
[65] M. Ablikim et al. (BES), eConf **C070805**, 02 (2007), [Phys. Lett.B660,315(2008)], 0705.4500
[66] M. Dimou, J. Lyon, R. Zwicky, Phys. Rev. **D87**, 074008 (2013), 1212.2242
[67] M. Beneke, G. Buchalla, M. Neubert, C.T. Sachrajda, Eur. Phys. J. **C61**, 439 (2009), 0902.4446
[68] G. Hiller, R. Zwicky, JHEP **03**, 042 (2014), 1312.1923
[69] S. Descotes-Genon, L. Hofer, J. Matias, J. Virto, JHEP **06**, 092 (2016), 1510.04239
[70] S. Descotes-Genon, J. Matias, J. Virto, Phys. Rev. **D88**, 074002 (2013), 1307.5683
[71] W. Altmannshofer, D.M. Straub, Eur. Phys. J. **C73**, 2646 (2013), 1308.1501
[72] T. Hurth, F. Mahmoudi, S. Neshatpour, Nucl. Phys. **B909**, 737 (2016), 1603.00865
[73] W. Altmannshofer, D.M. Straub, *Implications of $b \to s$ measurements*, in *Proceedings, 50th Rencontres de Moriond Electroweak Interactions and Unified Theories: La Thuile, Italy, March 14-21, 2015* (2015), pp. 333–338, 1503.06199, http://inspirehep.net/record/1353682/files/arXiv:1503.06199.pdf
[74] B. Capdevila, S. Descotes-Genon, L. Hofer, J. Matias, in preparation
[75] A.J. Buras, J. Girrbach, JHEP **12**, 009 (2013), 1309.2466
[76] R. Gauld, F. Goertz, U. Haisch, JHEP **01**, 069 (2014), 1310.1082
[77] A.J. Buras, F. De Fazio, J. Girrbach, JHEP **02**, 112 (2014), 1311.6729
[78] W. Altmannshofer, S. Gori, M. Pospelov, I. Yavin, Phys. Rev. **D89**, 095033 (2014), 1403.1269
[79] A. Celis, J. Fuentes-Martin, M. Jung, H. Serodio, Phys. Rev. **D92**, 015007 (2015), 1505.03079
[80] A. Falkowski, M. Nardecchia, R. Ziegler, JHEP **11**, 173 (2015), 1509.01249
[81] A. Crivellin, G. D'Ambrosio, J. Heeck, Phys. Rev. Lett. **114**, 151801 (2015), 1501.00993
[82] A. Crivellin, G. D'Ambrosio, J. Heeck, Phys. Rev. **D91**, 075006 (2015), 1503.03477
[83] S.M. Boucenna, A. Celis, J. Fuentes-Martin, A. Vicente, J. Virto, JHEP **12**, 059 (2016), 1608.01349
[84] A. Crivellin, J. Fuentes-Martin, A. Greljo, G. Isidori (2016), 1611.02703
[85] G. Hiller, M. Schmaltz, Phys. Rev. **D90**, 054014 (2014), 1408.1627
[86] B. Gripaios, M. Nardecchia, S.A. Renner, JHEP **05**, 006 (2015), 1412.1791
[87] D. Becirevic, S. Fajfer, N. Kosnik, Phys. Rev. **D92**, 014016 (2015), 1503.09024
[88] I. de Medeiros Varzielas, G. Hiller, JHEP **06**, 072 (2015), 1503.01084
[89] S. Fajfer, N. Kosnik, Phys. Lett. **B755**, 270 (2016), 1511.06024

[90] D. Becirevic, S. Fajfer, N. Kosnik, O. Sumensari, Phys. Rev. **D94**, 115021 (2016), 1608.08501
[91] B. Gripaios, M. Nardecchia, S.A. Renner, JHEP **06**, 083 (2016), 1509.05020
[92] M. Bauer, M. Neubert, Phys. Rev. Lett. **116**, 141802 (2016), 1511.01900
[93] P. Arnan, L. Hofer, F. Mescia, A. Crivellin (2016), 1608.07832
[94] G. Belanger, C. Delaunay, S. Westhoff, Phys. Rev. **D92**, 055021 (2015), 1507.06660
[95] W. Altmannshofer, I. Yavin, Phys. Rev. **D92**, 075022 (2015), 1508.07009
[96] W. Altmannshofer, M. Carena, A. Crivellin, Phys. Rev. **D94**, 095026 (2016), 1604.08221
[97] C. Bobeth, A.J. Buras, A. Celis, M. Jung (2016), 1609.04783
[98] A. Greljo, G. Isidori, D. Marzocca, JHEP **07**, 142 (2015), 1506.01705
[99] D. Becirevic, N. Kosnik, O. Sumensari, R. Zukanovich Funchal, JHEP **11**, 035 (2016), 1608.07583
[100] D.A. Faroughy, A. Greljo, J.F. Kamenik, Phys. Lett. **B764**, 126 (2017), 1609.07138